


Stepwise evolution of the Asian summer monsoon during the Holocene revealed by a stalagmite record from Heifeng Cave, Southwest China

The Holocene
1–9
© The Author(s) 2022
Article reuse guidelines:
sagepub.com/journals-permissions
DOI: 10.1177/09596836221074032
journals.sagepub.com/home/hol


Yingran Yan,^{1,2}  Xunlin Yang,^{1,2}  Rui Zhang,³
Riping Zhang,²  Saisi Zuli,²  and Yong Wang²

Abstract

The abrupt changes of the Asian summer monsoon (ASM) during the Holocene have long been of interest to environmental scientists. Here, RAMPFIT and Bayesian Change Point (BCP) analyses are applied to analyze the stalagmite $\delta^{18}\text{O}$ record from Heifeng Cave in southern China, and the results show that it is characterized by a distinct stepwise pattern of variation which can be divided into six stages (Stages, S) and five transitional phases (Transitions, T). In the early Holocene, when Northern Hemisphere summer insolation (NHSI) was at its maximum, the ASM underwent step-like increases in strength, comprising two stages. With the decrease in NHSI during the middle to late-Holocene, the weakening of ASM intensity was characterized by further step-like changes comprising three stages. The transitional phases of the monsoon are broadly correlative with millennial-scale monsoon weakening events associated with Bond events in the North Atlantic region, suggesting that the stepwise evolution of the ASM during the Holocene was caused by the combined effects of changes in NHSI and Bond events. We propose that Bond events may have acted as triggers that caused the ASM to cross a critical threshold, prompting a shift from one regime to another.

Keywords

ASM, Bond events, Holocene, stalagmite, step-like pattern, threshold effect

Received 5 September 2021; revised manuscript accepted 1 December 2021

Introduction

The rainfall delivered by the Asian summer monsoon (ASM) affects the livelihood and wellbeing of billions of people (Levermann et al., 2009). The variability of Holocene ASM was closely related to the development of human society and has attracted much research attention, with the instability of ASM being a focus. The DA stalagmite oxygen isotope record from Dongge Cave in China shows that the evolution of the ASM during the past 9000 years was interrupted by eight decadal- to centennial-scale weak monsoon events, six of which were related to well-documented ice-rafted detritus (IRD) events in the North Atlantic (Wang et al., 2005). Dykoski et al. (2005) noted that the intensity of the ASM decreased in a stepwise manner during the middle to late-Holocene, and proposed a threshold effect for monsoon intensity as an explanation. Donges et al. (2015) identified four non-linear regime shifts (NRS) in the Holocene evolution of the Asian monsoon, based on Recurrence Network analysis of several Asian speleothem records, which corresponded to episodes of rapid climate change (RCC) (Mayewski et al., 2004) and Bond events (Bond et al., 2001). A speleothem record from northeast China also showed that the ASM weakened in a step-like manner during the transition between the middle and late-Holocene, which affected cultural development within its region of influence (Zhao et al., 2021).

Previous studies of various geological archives have shown that gradual and low-amplitude climate changes, or non-linear

feedbacks, may lead to abrupt climate change when a certain threshold is reached (e.g. Claussen et al., 1999; Liu et al., 2006; Zhao et al., 2017). The gradual reduction of insolation (Levermann et al., 2009; Schewe et al., 2012; Zickfeld et al., 2005) and the resulting non-linear vegetation-atmosphere feedback processes (Claussen et al., 1999) are likely to have created a threshold effect in climate and ecosystem change. Zhao et al. (2017) demonstrated the occurrence of two significant abrupt changes in the vegetation of Central Asia during the Holocene, which may be attributed to the threshold effect of vegetation in response to orbitally-driven gradual climatic changes. Zickfeld et al. (2005) and Levermann et al. (2009) used a theoretical model of the monsoon to identify two regimes of monsoon stability during the

¹Chongqing Key Laboratory of Karst Environment, Southwest University, China

²Chongqing Jinpo Mountain Karst Ecosystem National Observation and Research Station, School of Geographical Sciences, Southwest University, China

³Institute of Global Environmental Change, Xi'an Jiaotong University, China

Corresponding author:

Xunlin Yang, Chongqing Key Laboratory of Karst Environment, School of Geographical Sciences, Southwest University, No. 2 Tiansheng Road, BeiBei District, Chongqing 400715, China.
Email: xlyang@swu.edu.cn

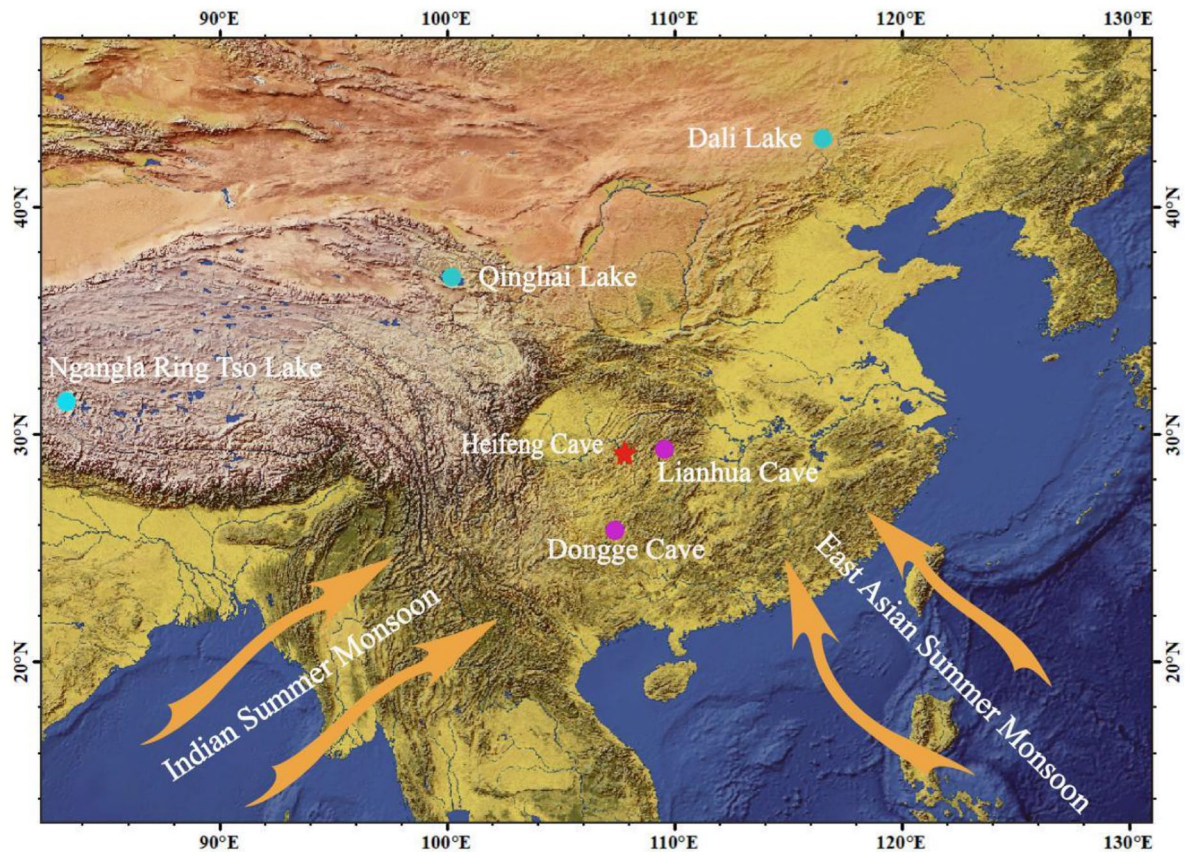


Figure 1. Topography and monsoon circulation in East Asia. The orange arrows show the trajectories of the East Asian summer monsoon (EASM) and the Indian summer monsoon (ISM). The red star shows the location of Heifeng Cave (Yang et al., 2019); the purple dots show the locations of Lianhua Cave (Zhang et al., 2016) and Dongge Cave (Dykoski et al., 2005); and the light blue dots show the locations of Dali Lake (Goldsmith et al., 2017), Qinghai Lake (An et al., 2012) and Ngangla Ring Tso Lake (Hudson et al., 2015).

Holocene. Pre-industrial variations in insolation and atmospheric greenhouse gas concentration may have driven the monsoon system to exceed certain thresholds or tipping points (Zickfeld et al., 2005), which triggered abrupt transitions between monsoon regimes (Levermann et al., 2009; Zickfeld et al., 2005). During these transitions the monsoon shifted abruptly and discontinuously from wet to dry stable states as insolation forcing caused a critical threshold to be exceeded (Boos and Storelvmo, 2016). Although the threshold effect has been discussed based on theoretical models of monsoon dynamics (Levermann et al., 2009; Schewe et al., 2012; Zickfeld et al., 2005), there is a lack of speleothem records of abrupt changes and threshold effects of the ASM during the Holocene.

Against this background, we use RAMPFIT to analyze the stalagmite HF01 record from Heifeng Cave in the middle to upper reaches of the Yangtze River in China to explore the abrupt changes of the Holocene Asian monsoon. Together with records from other sites in China we use the results to assess whether a step-like pattern of variation of the ASM during the Holocene is widely recorded, together with the possible driving mechanism.

Site, materials, and methods

Stalagmite HF01 was collected from Heifeng Cave (29°02'N, 107°11'E) in Jinfo Mountain, Chongqing City, at an altitude of 2130 m (Figure 1). The study area is located in the eastern Sichuan Basin, north of the Yunnan-Guizhou Plateau. Climatically, the region is controlled by the ASM (Zhang et al., 2021), and it has a humid subtropical monsoon climate with annual average temperature of 8.5°C and annual precipitation of ~1400 mm (Zhang et al., 2017). The ^{230}Th ages of the 30 samples from stalagmite HF01 are listed in Supplemental Table S1. No age

inversion is evident in the age sequence. The dating errors are small, mostly within 70 a, and therefore the chronology is highly reliable. The age model for stalagmite HF01 was established using MOD-AGE software (Hercman and Pawlak, 2012) (Supplemental Figure S1), and it indicates that the stalagmite grew uniformly, with the average rate of 1.13 mm/100 a.

The $\delta^{18}\text{O}$ record from stalagmite HF01 from Heifeng Cave spans the interval from 1.5 ka to 0.48 ka B.P. (thousands of years before 1950 CE), with an average resolution of 34 a. The $\delta^{18}\text{O}$ values of stalagmite HF01 range from -6.37‰ to -10.34‰ , with the mean of -8.81‰ , and the amplitude of variation is relatively large, reaching -3.71‰ . The most depleted part of the record is in the early and middle Holocene, when the $\delta^{18}\text{O}$ values vary greatly, with the mean value reaching the most depleted level (Figure 2). Yang et al. (2019) constructed an integrated Holocene record based on the $\delta^{18}\text{O}$ records of 16 stalagmites from the Asian monsoon domain, and concluded that the principal modes of the Holocene stalagmite $\delta^{18}\text{O}$ records and the instability of climate in the early Holocene. However, the monsoon characteristics reflected by HF01 $\delta^{18}\text{O}$ record that was one of the $\delta^{18}\text{O}$ records of 16 stalagmites have not been thoroughly analyzed (Yang et al., 2019). Therefore, based on the HF01 $\delta^{18}\text{O}$ record, RAMPFIT and Bayesian Change Point (BCP) analyses are used to discuss further the evolution of ASM in the Holocene in this paper (Mudelsee, 2000; Ruggieri, 2013).

RAMPFIT is a statistical regression approach (Mudelsee, 2000) which has been widely used in paleoclimate reconstruction (e.g. Fleitmann et al., 2003; Jiang et al., 2012; Li et al., 2021; Steffensen et al., 2008; Zhang et al., 2019), and we used it to determine change points in the stalagmite HF01 $\delta^{18}\text{O}$ sequence. RAMPFIT involves fitting a “ramp” to a specific part of a record using a weighted least squares method, and it can be used to

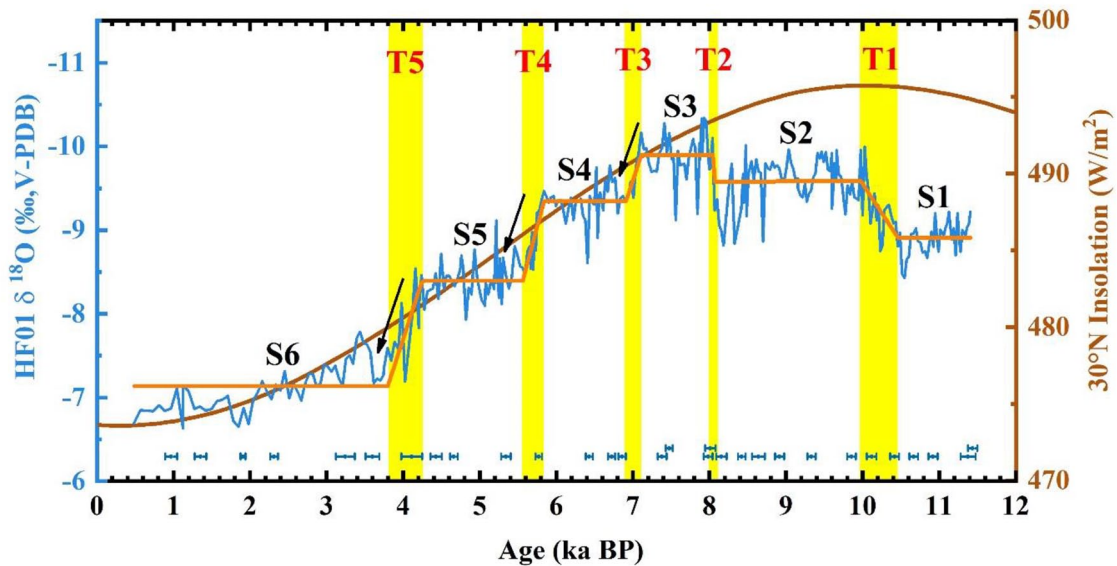


Figure 2. The $\delta^{18}\text{O}$ record of stalagmite HF01. The blue curve represents the HF01 $\delta^{18}\text{O}$ record (Yang et al., 2019), with the error bars indicating the dating error ($\pm 2\sigma$); the brown curve represents summer insolation at 30°N (Laskar et al., 2004); and the orange curve represents the results of RAMPFIT analysis (Mudelsee, 2000). The yellow vertical bars indicate transitional phases (T1–T5) of the monsoon regime.

determine the exact age of climate change points and the average state before and after a change (Mudelsee, 2000) (Figure 2, Supplemental Table S2). According to the trend of variation of the HF01 $\delta^{18}\text{O}$ record, we divided the record into several intervals and piecewise fitted the data; no changes were made to the location of change points in the fitting curve. Finally, we integrated the results of multi-segment fitting into a complete and continuous record. In order to verify whether the division of segments in the $\delta^{18}\text{O}$ record was objective and reasonable, Acycle software was used to perform Bayesian Change Point analysis (Li et al., 2019; Ruggieri, 2013) (Supplemental Figure S2 and Table S3). Based on a Bayesian mathematical algorithm, the method can be used to estimate the number of change points in a time series and the uncertainty probability of the change point locations (Ruggieri, 2013). PAST software was then used to perform wavelet analysis of the $\delta^{18}\text{O}$ record in order to identify the dominant cycles in the ASM during the Holocene (Hammer et al., 2001).

Discussion

Stepwise evolution of the ASM during the Holocene

The RAMPFIT results for stalagmite HF01 indicate that the evolution of the ASM during the Holocene was non-linear and step-like (Mudelsee, 2000) (Figure 2). The evolution can be divided into six stable stages (Stages, S) and five transitional phases (Transitions, T). Each stage is equivalent to a plateau with roughly constant $\delta^{18}\text{O}$ values, suggesting a relatively stable monsoon state; and each stage is separated by a transitional phase, characterized by a large shift in $\delta^{18}\text{O}$, indicating an abrupt change in the monsoon regime. There are two stages (S1, S2) and two transitional phases (T1, T2) in the early and middle Holocene, and there are four stages (S3–S6) and three transitional phases (T3–T5) in the middle to late-Holocene. The entire late-Holocene falls within the weak monsoon stage (S6). The results of RAMPFIT analysis are highly consistent with the model output obtained using the BCP algorithm (Mudelsee, 2000; Ruggieri, 2013) (Figures 2 and Supplemental Figure S2). Transition T2 has the highest posterior probability, reaching 71%, while transitions T1 (51%), T4 (59%) and T5 (40%) all have a posterior probability of $\sim 50\%$ (Supplemental Figure S2). Therefore, supported by the BCP analysis, the results of the RAMPFIT analysis of the HF01 $\delta^{18}\text{O}$ record are deemed reliable.

Modern cave monitoring studies in the Jinfo Mountain area have shown that $\delta^{18}\text{O}$ in cave drip water inherits the signal of the interannual variation of stable isotopes in precipitation, and is sensitive to changes in atmospheric circulation and ENSO mode (Chen and Li, 2018). As a consequence, we argue that the $\delta^{18}\text{O}$ of stalagmite HF01 can provide insights into the variation of ASM intensity on a large spatial scale, with more depleted/enriched $\delta^{18}\text{O}$ values indicating an increase/decrease in ASM intensity, as has been shown in Yang et al. (2019). The HF01 $\delta^{18}\text{O}$ record of the early Holocene can be divided into two stages: (1) In the first stage (S1, 11.41–10.46 ka B.P.) the average $\delta^{18}\text{O}$ is -8.90% , and the values are relatively uniform, indicating that the ASM was stable state with a moderate intensity. (2) In the second stage (S2, 9.97–8.07 ka B.P.), which lasted for almost 2 ka, the average $\delta^{18}\text{O}$ value is -9.57% . Notably, the $\delta^{18}\text{O}$ record shows a centennial-scale “W”-shaped oscillation during the transitional period (8.5–8.1 ka B.P.) between the early and middle Holocene (Yang et al., 2020). This oscillation corresponds the well-documented 8.2 ka event (Alley et al., 1997; Cheng et al., 2009), which interrupted the continuous strengthening of the ASM, indicating that the ASM was unstable in the early Holocene (Yang et al., 2019, 2020).

The HF01 $\delta^{18}\text{O}$ record for the middle Holocene shows a pronounced enrichment trend, with three stages and three intervening steps: (1) In the first stage of the middle Holocene (S3, 8.04–7.11 ka B.P.), the $\delta^{18}\text{O}$ values are the most depleted in the Holocene, with an average of -9.90% , indicating that the ASM reached a state of maximum intensity (Figure 2). The variation of the ASM intensity during the Holocene was mainly controlled by changes in NHSI (Wang et al., 2005; Zhang et al., 2019), but there was a lag of 2–3 ka between the maximum negative inflection in $\delta^{18}\text{O}$ and the maximum in NHSI (Laskar et al., 2004) (Figure 2). This may have been caused by the large global ice volume in the early Holocene (Fleitmann et al., 2003), which delayed the onset of the Holocene climatic optimum (Bakker et al., 2016; Ruddiman, 2006). (2) In the second stage of the middle Holocene (S4, 6.90–5.84 ka B.P.), the $\delta^{18}\text{O}$ values are moderately depleted and relatively stable (Yang et al., 2019) (Figure 2), with an average of -9.34% , suggesting that the ASM remained relatively strong compared to S1. (3) In the third stage of the middle Holocene (S5, 5.56–4.31 ka B.P.), the $\delta^{18}\text{O}$ values are substantially more enriched than S4, with an average of -8.43% , suggesting that the

Table 1. Locations of caves and lakes from monsoonal China used in this study.

No.	Site	Location	Altitude (m a.s.l.)	Reference
1	Dali Lake	43°09'N, 116°17'E	1220	Goldsmith et al. (2017)
2	Qinghai Lake	36°32'–37°15'N, 99°36'–100°47'E	3194	An et al. (2012)
3	Ngangla Ring Tso Lake	31°27'–31°39'N, 82°48'–83°24'E	4727	Hudson et al. (2015)
4	Lianhua Cave	29°29'N, 109°32'E	455	Zhang et al. (2016)
5	Heifeng Cave	29°01'N, 107°11'E	2130	Yang et al. (2019)
6	Dongge Cave	25°02'N, 108°05'E	680	Dykoski et al. (2005)

ASM intensity had weakened significantly following the two sharp decreases (Figure 2). The HF01 $\delta^{18}\text{O}$ values showed an obvious and rapid enrichment change during the mid-late-Holocene transitional period (T5, 4.3–3.8 ka B.P.), and then emerged a slow enrichment change. The HF01 $\delta^{18}\text{O}$ reached the most enrichment in the period of 2–0.48 ka B.P., with an average of -6.95‰ , indicating that the ASM was relatively stable and the ASM intensity reached the lowest level in the Holocene (Figure 2).

Comparison of stalagmite HF01 record with other monsoon records

In order to determine whether the step-like characteristics of the Holocene ASM recorded by stalagmite HF01 are consistent on a large spatial scale, we compared the results with other Holocene climate records from the Asian monsoon region (see Table 1 and Figure 3). The lake-level record of Dali Lake in Inner Mongolia also shows a pronounced step-like pattern, with the period of highest lake level including two stable intervals (Goldsmith et al., 2017), during 6.3–5.8 and 8.2–7.3 ka B.P., in the middle Holocene, indicating that the strongest monsoon occurred at these times (Figure 3a). A record from Ngangla Ring Tso Lake, in the Tibetan Plateau, also shows that the lake level experienced a pronounced stepwise decrease from the early to the late-Holocene (Hudson et al., 2015) (Figure 3b). Moreover, the three major falls in lake level correspond exactly to the shifts in the monsoon regime (Figure 3b and d). The Summer Monsoon Index (SMI) from Qinghai Lake shows that the monsoon was unstable in the early Holocene, while stable stages occurred during 8.5–7.0 and 6.6–5.4 ka B.P., in the middle Holocene (An et al., 2012) (Figure 3c). The $\delta^{18}\text{O}$ record of stalagmite LHD5 from Lianhua Cave shows a stepwise pattern of variation with five stages during the Holocene (Zhang et al., 2016) (Figure 3e). The variation of LHD5 $\delta^{18}\text{O}$ record shows that the ASM strengthened rapidly at the beginning of the Holocene and subsequently remained strong and stable during 11.2–9.5 ka B.P. (Figure 3e). Maximum ASM intensity occurred during 9.5–7.0 ka B.P., which was followed by a stepwise weakening comprising three stages (Figure 3e). The $\delta^{18}\text{O}$ record of stalagmite D4 from Dongge Cave shows a stepwise pattern with five stages (Dykoski et al., 2005) (Figure 3f). The ASM oscillated substantially in the early Holocene and was relatively strong during 9.0–7.1 ka B.P.; and in the middle to late-Holocene, it shows a pronounced stepwise pattern with three stages (Figure 3f). The stalagmite records from Heifeng cave, Dongge cave (Dykoski et al., 2005), and Lianhua cave (Zhang et al., 2016) have obvious stepwise changes in the Holocene, but there are also some differences between them. The records of Heifeng cave have six steps, while Dongge cave and Lianhua cave have only five steps, which may indicate that the stalagmite $\delta^{18}\text{O}$ from Heifeng cave at higher altitude are more sensitive to the changes of ASM.

Lake records (An et al., 2012; Goldsmith et al., 2017) and speleothem records (Dykoski et al., 2005; Zhang et al., 2016) from Chinese monsoon region reveal differences in the stepwise

enhancement of the ASM in the early Holocene (Figure 3), suggesting that the ASM variability in the early Holocene was complex and unstable (Yang et al., 2019). Even though NHSI was at a maximum in the early Holocene (Laskar et al., 2004), the ice volume in the Northern Hemisphere was still large (Fleitmann et al., 2003), and the enhancement of ASM was probably constrained by glacial background conditions (Liu et al., 2018b). What's more, the disturbances of fresh water discharge resulted in an unstable ASM (Bond et al., 2001; Yang et al., 2019). In addition, the principal modes of the ASM in the Asian monsoon region were similar during the middle to late-Holocene, showing a typical stepwise pattern with three stages of weakening, which is consistent with the gradual weakening of NHSI from a maximum to a minimum (Laskar et al., 2004; Yang et al., 2019). Previous studies have shown the cold and dry climatic events in the middle to late-Holocene were transmitted across middle to low latitudes of the Northern Hemisphere and the resulting monsoon-weakening events were important causes of a worldwide decline of prehistoric civilizations and ethnic migrations at this time (Arz et al., 2006; Booth et al., 2005; Gasse, 2000; Shao et al., 2006). For example, the demise of Neolithic civilizations in Central China (Wu and Liu, 2004; Yang et al., 2021), the Mesopotamian civilization (deMenocal, 2001), and civilizations in India (Dalfes et al., 1997) may have been linked to these events.

Mechanism of the stepwise evolution of the Holocene ASM

The long-term trend of the $\delta^{18}\text{O}$ record from stalagmite HF01 essentially tracks the variation of NHSI during the Holocene (Laskar et al., 2004) (Figure 2), indicating that the NHSI is the dominant driver of the ASM on the orbital scale (Dykoski et al., 2005; Wang et al., 2005; Zhang et al., 2019). However, a series of centennial- and millennial-scale abrupt events are superimposed on this main trend. These abrupt climatic events essentially correspond to the NRS defined by Donges et al. (2015) (Supplemental Figure S3). During the intervals of 10.9–10.5, 9.9–9.7, 9.4–9.1, 8.4–8.1, 7.4–7.1, 5.9–5.5, and 4.3–3.9 ka B.P., the HF01 $\delta^{18}\text{O}$ record shows varying degrees of positive shifts, corresponding to 7 weak monsoon events. Five of these events mainly occurred during transitional phases (T1–T5) of the ASM. These events are not only consistent with episodes of rapid climate change (RCC) during the Holocene (Mayewski et al., 2004), but they also coincide with Bond events (Bond et al., 2001) (Figure 4d and e, Supplemental Figure S3), which suggests that the Bond events may have acted as a trigger that prompted the ASM to switch from one regime to another.

During the early to middle Holocene, the weak ASM events corresponding to Bond events 8–5 were considered as the results of the combined effect of the Atlantic Meridional Overturning Circulation (AMOC) and solar output (Cheng et al., 2009; Liu et al., 2018b, 2020; Zhang et al., 2018). The transitional phases T1 and T2 in the HF01 $\delta^{18}\text{O}$ record coincide with Bond events 8 and 5, respectively (Figure 4d and e). These two events

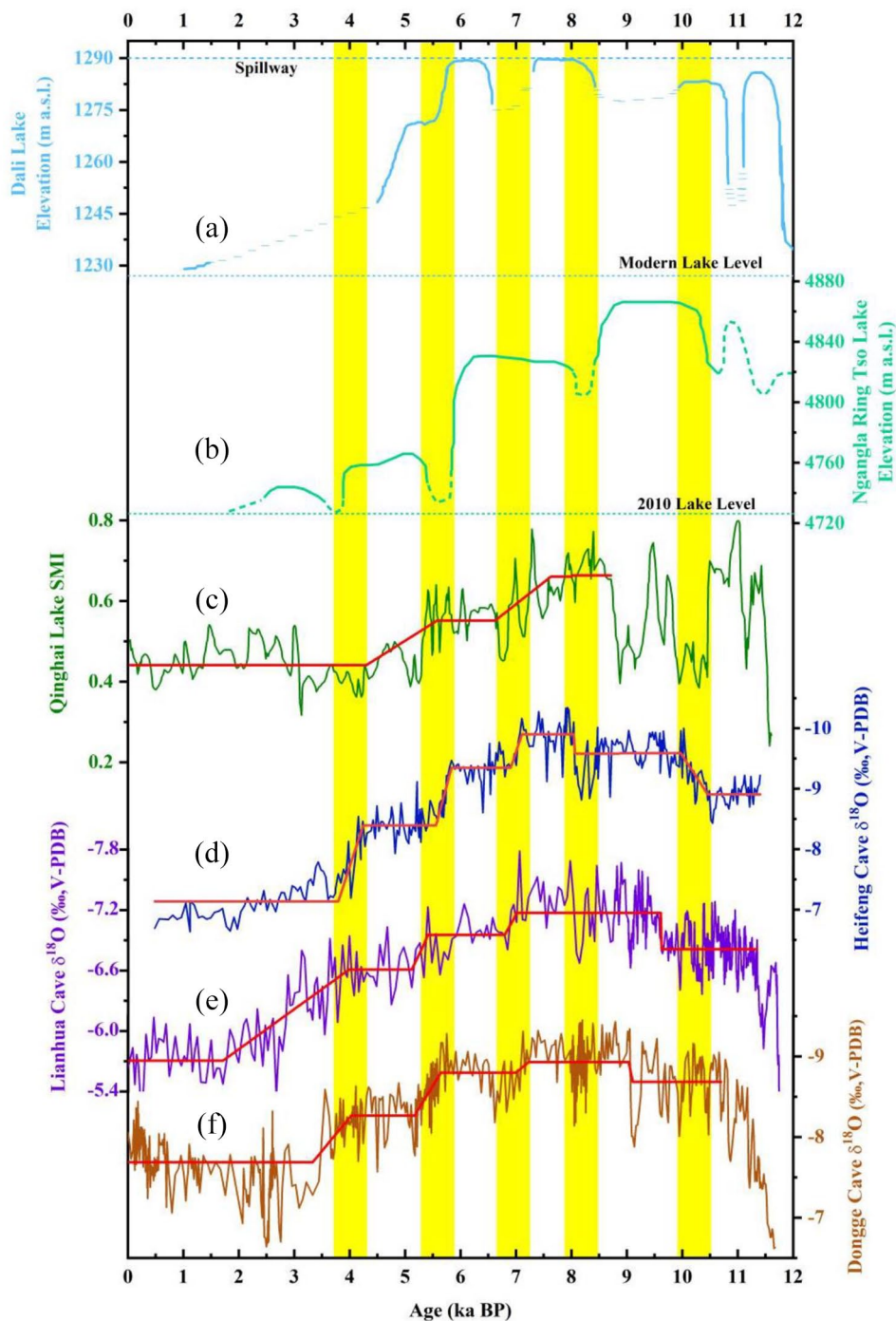


Figure 3. Comparison of the stalagmite HF01 $\delta^{18}\text{O}$ record with other climate records from the Asian monsoon region. (a) Lake level record of Dali Lake (Goldsmith et al., 2017). (b) Lake level record of Ngangla Ring Tso Lake (Hudson et al., 2015). (c) Summer Monsoon Index (SMI) from Qinghai Lake (An et al., 2012). (d) $\delta^{18}\text{O}$ record of stalagmite HF01 from Heifeng Cave (Yang et al., 2019). (e) $\delta^{18}\text{O}$ record of stalagmite LHD5 from Lianhua Cave (Zhang et al., 2016). (f) $\delta^{18}\text{O}$ record of stalagmite D4 from Dongge Cave (Dykoski et al., 2005); Red solid lines represent RAMPFIT results, and the yellow vertical bars represent abrupt monsoon transitional phases.

interrupted the strengthening process of the ASM (Yang et al., 2019), and each transitional phase was rapidly followed by a stage of rapid monsoon strengthening, respectively reaching a peak and sub-peak in ASM intensity. This may be attributed to the fact that NHSI was strong in the early Holocene (Figure 4a), and the consequent Northern Hemisphere warming caused a northward shift of the Intertropical Convergence Zone (ITCZ) (Haug et al., 2001), resulting in the continuous strengthening of ASM. However, the Bond events disrupted the relatively stable monsoon states (Liu et al., 2018a), promoting a non-linear shift in ASM intensity after the end of each weak monsoon event. The ASM before and during the Bond event 8 was probably

constrained by glacial background conditions (Liu et al., 2018b). The HF01 $\delta^{18}\text{O}$ record shows that when the weak ASM event corresponding to Bond event 7 came to the end, ASM shifted rapidly from S1 to S2 (Figure 4d and e), which suggests that the constraining effect of averaged climate state on the ASM was alleviated (Liu et al., 2018b). However, the weak monsoon event, corresponding to the Bond event 6, did not promote a monsoon shift from one regime to a stronger one, which may be due to the fact that ASM had just gone through T1 at this point and its intensity had not yet reached the next critical threshold.

In the middle to late-Holocene, the three transitional phases of the monsoon regime (T2, T4, and T5) correspond precisely to

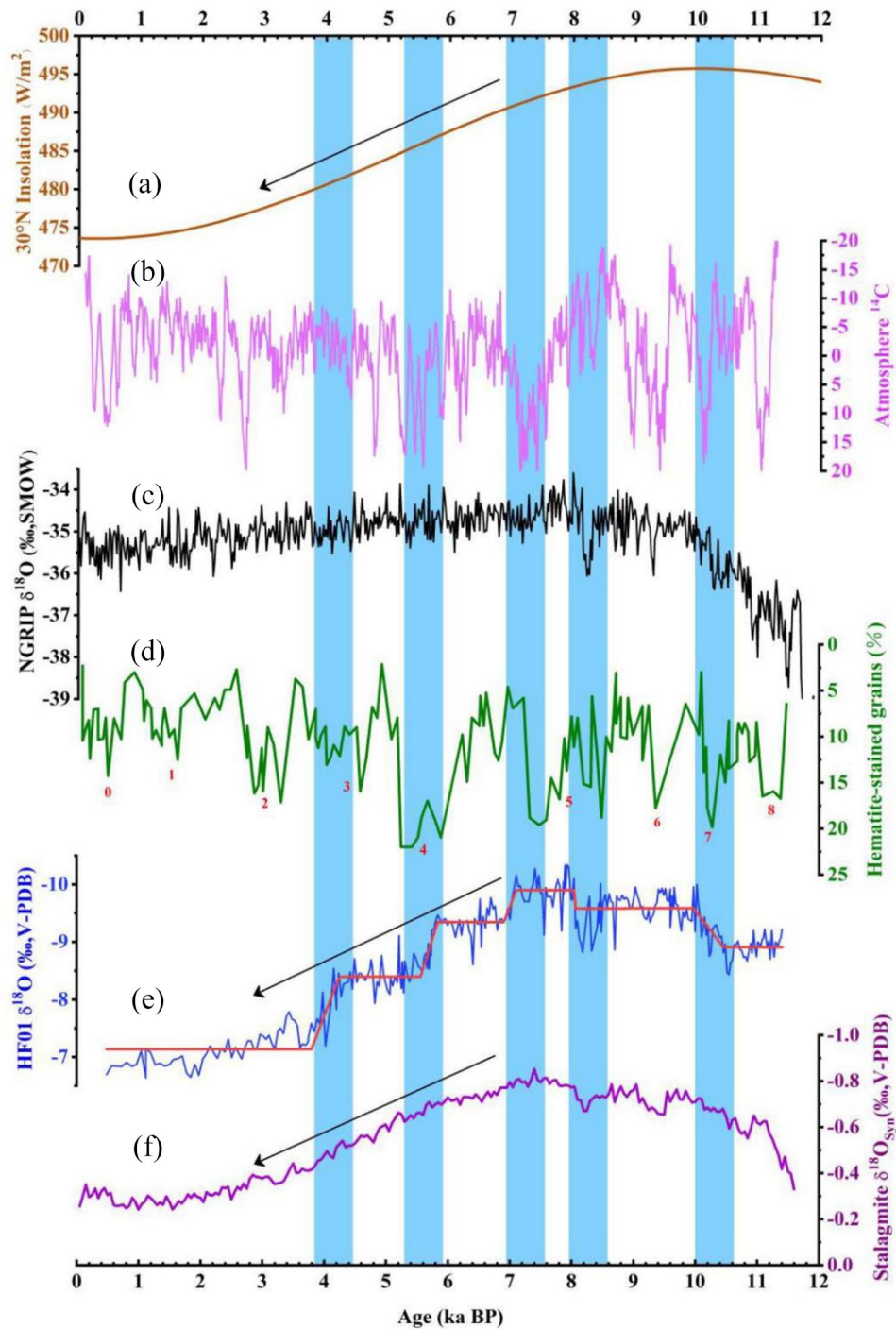


Figure 4. Comparison of Holocene weak monsoon events with Bond events in the North Atlantic. (a) Summer insolation at 30°N (Laskar et al., 2004). (b) Atmospheric ^{14}C production rate record (Reimer et al., 2013). (c) Greenland ice core $\delta^{18}\text{O}$ record (Johnsen et al., 2001). (d) Ice-rafted detritus (IRD) record from the North Atlantic (Bond et al., 2001); the red numbers correspond to Bond events. (e) $\delta^{18}\text{O}$ record of stalagmite HF01 (Yang et al., 2019); the red solid line represents RAMPFIT results. (f) Synthesis Holocene stalagmite $\delta^{18}\text{O}_{\text{syn}}$ record from China (Yang et al., 2019). Light blue vertical bars represent weak monsoon events that correspond to Bond events.

Bond events 5, 4, and 3, respectively (Figure 4d and e). Due to the relatively long duration of Bond event 5 (Bond et al., 2001), it is likely that the 7.2 ka weak monsoon event, corresponding to T3, was also the result of the weakening of the AMOC (Feng et al., 2020). Different from the early Holocene, during the middle to late-Holocene, the ASM weakened substantially in a stepwise manner with no recovery. Accompanied by the gradual decrease of NHSI during the middle to late-Holocene (Laskar et al., 2004) (Figure 4a), the so-called positive feedback of moisture-advection dominated the continent-ocean heat balance (governed by latent heat) of the AM system (Levermann et al., 2009; Schewe et al., 2012). When the positive feedback of moisture-advection

strengthened continuously, the monsoon intensity would enhance to gradually approach the threshold of abrupt change (Schewe et al., 2012). After the end of weak monsoon events corresponding to triggered by Bond events, the ASM dropped to a weaker but stable state (Figure 4e). However, the intensity of the ASM did not recover to its original level, which may have been directly related to the weakening of NHSI. With the gradual decrease of NHSI, the cooling of the Northern Hemisphere resulted in a southward shift of the ITCZ (Haug et al., 2001), and therefore the intensity of the ASM failed to regain its previous level. The foregoing scenario suggests a close and complex relationship between insolation, the threshold effect of abrupt monsoon change, and

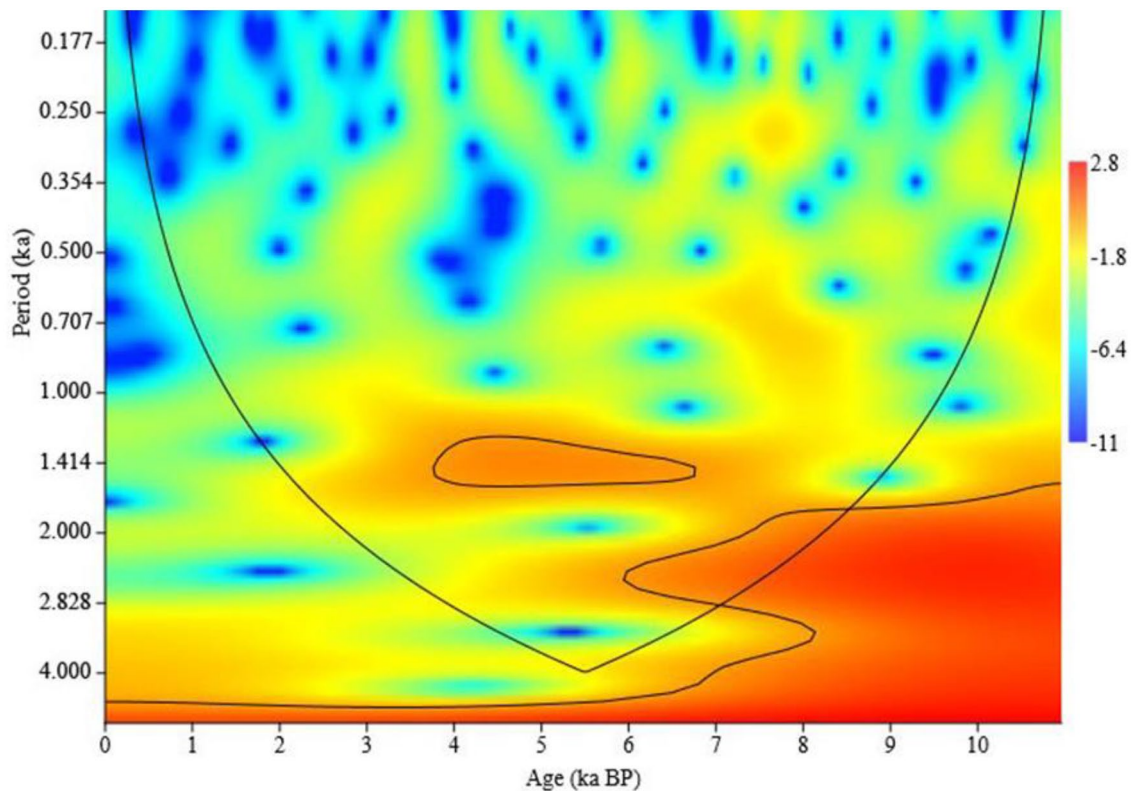


Figure 5. Wavelet analysis results for the $\delta^{18}\text{O}$ record of stalagmite HF01.

Bond events, in the course of the overall process of monsoon climate change during the Holocene.

As the precursors of transitional phases, these pronounced weak monsoon events differ from Bond events in terms of structure (Figure 4d and e). Bond events occurred repeatedly during the Holocene, and the temperature recovered after the end of each event, resulting in a symmetrical pattern of cooling and subsequent warming (Bond et al., 2001). However, the weakening and strengthening phases of the ASM, as revealed in the $\delta^{18}\text{O}$ record from stalagmite HF01, are asymmetrical, which is confirmed by the synthesis of stalagmite records from 14 caves in the Asian monsoon region (Yang et al., 2019) (Figure 4f). There were three pronounced weak monsoon events in the early Holocene, but there is no evidence of similar weak monsoon events in the middle to late-Holocene (Yang et al., 2019). This may be due to the fact that the weakening of ASM was monotonic in the middle to late-Holocene, with no recovery process, which resulted in these events being smoothed out in the stacked record comprising multiple curves.

Previous studies have shown that there is a teleconnection between the weak ASM events and the North Atlantic Bond events (Cheng et al., 2009; Liu et al., 2013; Liu et al., 2020; Wang et al., 2005). The global coupled ocean-atmosphere model (CM2.0) shows that the freshwater forcing substantially weakens the Atlantic Thermohaline Circulation (THC), resulting in a southward shift of the ITCZ over the Atlantic and Pacific, an El Niño-like pattern in the southeastern tropical Pacific, and weakened Asian summer monsoons through air-sea interactions (Zhang and Delworth, 2005).

The stalagmite HF01 $\delta^{18}\text{O}$ record further shows that stepwise evolution of Holocene ASM was probably driven jointly by NHSI and Bond events (Figure 4), and not every Bond event can trigger a change in the monsoon regime. The comparison between the atmospheric ^{14}C production rate record and HF01 record revealed that solar activity also played a role in the transitions of ASM regimes such as T1, T3, and T4 (Reimer et al., 2013) (Figure 4b and e). On the orbital scale, the gradual change in NHSI may have

caused the monsoon system to approach a critical state (deMenocal et al., 2000; Dykoski et al., 2005). It is likely that Bond events acted as a trigger of the threshold effect and was a key driving force for the transition of the ASM from one regime to another; moreover, the internal feedback of the monsoon system may have amplified this external forcing (Levermann et al., 2009). At present, the threshold of NHSI and trigger mechanism are still unclear, and further research is needed. Schewe et al. (2012) speculated that orbital-timescale variations in NHSI and the associated surface temperature changes might have affected evaporation at the ocean's surface, such that average humidity over the ocean persistently crossed the threshold, thus critically altering the moisture supply for the adjacent monsoon region and triggering a transition between the two regimes.

The results of wavelet analysis reveal a 1.45 ka cycle in the HF01 stalagmite $\delta^{18}\text{O}$ (Figure 5), which is close to the 1.5 ka cycle of North Atlantic climate change (Bianchi and McCave, 1999; Bond et al., 1997). This common periodicity in records from the North Atlantic and the ASM region points to a teleconnection between climate change in the two climatic regions (Gupta et al., 2005), and further confirms a relationship between the stepwise pattern of variation of the ASM during the Holocene and the centennial- to millennial-scale cold events in the North Atlantic, suggesting that Bond events were important factors that triggered major changes in the ASM.

Conclusions

Based on a high-resolution $\delta^{18}\text{O}$ record from stalagmite HF01 from Heifeng Cave in southern China and other paleoclimate records, we have reconstructed the evolution of the ASM during the Holocene (~11.5–0.48 ka B.P.). The following conclusions are drawn.

- (1) The results of RAMPFIT and BCP analysis of the $\delta^{18}\text{O}$ record show that the evolution of the ASM during the Holocene was characterized by a stepwise pattern, which

can be divided into six stages separated by five transitional phases.


- (2) The Holocene variation of the ASM is consistent with the weakening of NHSI on the orbital scale, indicating that NHSI was a major driver of the ASM. Due to the strong NHSI in the early Holocene, the ASM intensity underwent two stages of enhancement in the early Holocene, followed by three stages of weakening in the middle to late-Holocene, as NHSI gradually weakened.
- (3) The HF01 $\delta^{18}\text{O}$ record shows that the transitional phases of the ASM regime are consistent with Bond events in the North Atlantic. Additionally, wavelet analysis reveals the presence of a 1.45 ka cycle in the HF01 $\delta^{18}\text{O}$ record, which is close to the well-documented 1.5 ka cycle of North Atlantic climate change, suggesting that Bond events may have acted as a trigger for the transition of one ASM state to another.

Funding

The author(s) disclosed receipt of the following financial support for the research, authorship, and/or publication of this article: This work was supported by grants from the National Natural Science Foundation of China (41971109 and 41572158), National Key R&D Program of China (2016YFC0502301).

ORCID iDs

Yingran Yan  <https://orcid.org/0000-0001-5533-7733>

Xunlin Yang  <https://orcid.org/0000-0002-8259-4206>

Riping Zhang  <https://orcid.org/0000-0002-3442-5678>

Saisi Zuli  <https://orcid.org/0000-0003-4155-8193>

Supplemental material

Supplemental material for this article is available online.

References

- Alley RB, Mayewski PA, Sowers T et al. (1997) Holocene climatic instability: A prominent, widespread event 8200 yr ago. *Geology* 25: 483–486.
- An Z, Colman SM, Zhou W et al. (2012) Interplay between the Westerlies and Asian monsoon recorded in Lake Qinghai sediments since 32 ka. *Scientific Reports* 2(8): 619.
- Arz HW, Lamy F and Paetzold J (2006) A pronounced dry event recorded around 4.2 ka in brine sediments from the northern Red Sea. *Quaternary Research* 66: 432–441.
- Bakker P, Clark P, Golledge N et al. (2016) Centennial-scale Holocene climate variations amplified by Antarctic Ice Sheet discharge. *Nature* 541(7635): 72–76.
- Bianchi GG and McCave IN (1999) Holocene periodicity in North Atlantic climate and deep-ocean flow south of Iceland. *Nature* 397: 515–517.
- Bond G, Kromer B, Beer J et al. (2001) Persistent solar influence on north Atlantic climate during the Holocene. *Science* 294: 2130–2136.
- Bond G, Showers W, Cheseby M et al. (1997) A pervasive millennial-scale cycle in North Atlantic Holocene and glacial climates. *Science* 278: 1257–1266.
- Boos WR and Storelvmo T (2016) Near-linear response of mean monsoon strength to a broad range of radiative forcings. *Proceedings of the National Academy of Sciences of the United States of America* 113: 1510–1515.
- Booth RK, Jackson ST, Forman SL et al. (2005) A severe centennial-scale drought in mid-continental North America 4200 years ago and apparent global linkages. *Holocene* 15: 321–328.
- Chen C-J and Li T-Y (2018) Geochemical characteristics of cave drip water respond to ENSO based on a 6-year monitoring work in Yangkou Cave, Southwest China. *Journal of Hydrology* 561: 896–907.
- Cheng H, Fleitmann D, Edwards RL et al. (2009) Timing and structure of the 8.2 kyr BP event inferred from $\delta^{18}\text{O}$ records of stalagmites from China, Oman, and Brazil. *Geology* 37: 1007–1010.
- Claussen M, Kubatzki C, Brovkin V et al. (1999) Simulation of an abrupt change in Saharan vegetation in the mid-Holocene. *Geophysical Research Letters* 26: 2037–2040.
- Dalfes N, Kukla G and Weiss H (1997) *Third Millennium BC Climate Change and Old World Collapse*. NATO ASI Series, vol. 49. Berlin, Heidelberg: Springer-Verlag.
- deMenocal P, Ortiz J, Guilderson T, et al. (2000) Abrupt onset and termination of the African Humid Period: rapid climate responses to gradual insolation forcing. *Quaternary Science Reviews* 19: 347–361.
- deMenocal PB (2001) Cultural responses to climate change during the Late-Holocene. *Science* 292: 667–673.
- Donges JF, Donner RV, Marwan N et al. (2015) Non-linear regime shifts in Holocene Asian monsoon variability: Potential impacts on cultural change and migratory patterns. *Climate of the Past* 11: 709–741.
- Dykoski CA, Edwards RL, Cheng H et al. (2005) A high-resolution, absolute-dated Holocene and deglacial Asian monsoon record from Dongge Cave, China. *Earth and Planetary Science Letters* 233: 71–86.
- Feng X, Yang Y, Cheng H et al. (2020) The 7.2 ka climate event: Evidence from high-resolution stable isotopes and trace element records of stalagmite in Shuiming Cave, Chongqing, China. *Holocene* 30: 145–154.
- Fleitmann D, Burns SJ, Mudelsee M et al. (2003) Holocene forcing of the Indian monsoon recorded in a stalagmite from Southern Oman. *Science* 300: 1737–1739.
- Gasse F (2000) Hydrological changes in the African tropics since the Last Glacial Maximum. *Quaternary Science Reviews* 19: 189–211.
- Goldsmith Y, Broecker WS, Xu H et al. (2017) Northward extent of East Asian monsoon covaries with intensity on orbital and millennial timescales. *Proceedings of the National Academy of Sciences of the United States of America* 114: 1817–1821.
- Gupta AK, Das M and Anderson DM (2005) Solar influence on the Indian summer monsoon during the Holocene. *Geophysical Research Letters* 32(17): L17703.
- Hammer O, Harper D and Ryan P (2001) PAST: Paleontological statistics software package for education and data analysis. *Palaeontologia Electronica* 4: 1–9.
- Haug GH, Hughen KA, Sigman DM et al. (2001) Southward migration of the intertropical convergence zone through the Holocene. *Science* 293: 1304–1308.
- Hercman H and Pawlak J (2012) MOD-AGE: An age-depth model construction algorithm. *Quaternary Geochronology* 12: 1–10.
- Hudson AM, Quade J, Huth TE et al. (2015) Lake level reconstruction for 12.8–2.3 ka of the Ngangla Ring Tso closed-basin lake system, southwest Tibetan Plateau. *Quaternary Research* 83: 66–79.
- Jiang X, He Y, Shen C et al. (2012) Stalagmite-inferred Holocene precipitation in northern Guizhou Province, China, and asynchronous termination of the Climatic Optimum in the Asian monsoon territory. *Chinese Science Bulletin* 57: 795–801.
- Johnsen SJ, Dahl-Jensen D, Gundestrup N, et al. (2001) Oxygen isotope and palaeotemperature records from six Greenland ice-core stations: Camp Century, Dye-3, GRIP, GISP2, Renland and NorthGRIP. *Journal of Quaternary Science* 16(4): 299–307.
- Laskar J, Robutel P, Joutel F et al. (2004) A long-term numerical solution for the insolation quantities of the Earth. *Astronomy & Astrophysics* 428: 261–285.
- Levermann A, Schewe J, Petoukhov V et al. (2009) Basic mechanism for abrupt monsoon transitions. *Proceedings of the*

- National Academy of Sciences of the United States of America* 106: 20572–20577.
- Li M, Hinnov L and Kump L (2019) Acycle: Time-series analysis software for paleoclimate research and education. *Computers & Geosciences* 127: 12–22.
- Li T-Y, Wu Y, Shen C-C et al. (2021) High precise dating on the variation of the Asian summer monsoon since 37 ka BP. *Scientific Reports* 11(1): 9375.
- Liu D, Wang Y, Cheng H et al. (2018a) Contrasting patterns in abrupt Asian summer monsoon changes in the last glacial period and the Holocene. *Paleoceanography and Paleoclimatology* 33: 214–226.
- Liu SS, Liu DB, Wang YJ, et al. (2018b) Asian hydroclimate changes and mechanisms in the preboreal from an annually-laminated stalagmite, Daoguan Cave, Southern China. *Acta Geologica Sinica-English Edition* 92: 367–377.
- Liu X, Sun Y, Vandenberghe J et al. (2020) Centennial- to millennial-scale monsoon changes since the last deglaciation linked to solar activities and North Atlantic cooling. *Climate of the Past* 16: 315–324.
- Liu YH, Henderson GM, Hu CY et al. (2013) Links between the East Asian monsoon and North Atlantic climate during the 8,200 year event. *Nature Geoscience* 6: 117–120.
- Liu Z, Wang Y, Gallimore R et al. (2006) On the cause of abrupt vegetation collapse in North Africa during the Holocene: Climate variability vs. vegetation feedback. *Geophysical Research Letters* 33(22): L22709.
- Mayewski PA, Rohling EE, Stager JC et al. (2004) Holocene climate variability. *Quaternary Research* 62: 243–255.
- Mudelsee M (2000) Ramp function regression: A tool for quantifying climate transitions. *Computers & Geosciences* 26: 293–307.
- Reimer PJ, Bard E, Bayliss A et al. (2013) IntCal13 and Marine13 radiocarbon age calibration curves 0–50,000 years cal BP. *Radiocarbon* 55: 1869–1887.
- Ruddiman WF (2006) Orbital changes and climate. *Quaternary Science Reviews* 25: 3092–3112.
- Ruggieri E (2013) A Bayesian approach to detecting change points in climatic records. *International Journal of Climatology* 33: 520–528.
- Schewe J, Levermann A and Cheng H (2012) A critical humidity threshold for monsoon transitions. *Climate of the Past* 8: 535–544.
- Shao XH, Wang YJ, Cheng H et al. (2006) Long-term trend and abrupt events of the Holocene Asian monsoon inferred from a stalagmite $\delta^{18}\text{O}$ record from Shennongjia in Central China. *Chinese Science Bulletin* 51: 221–228.
- Steffensen JP, Andersen KK, Bigler M et al. (2008) High-resolution Greenland Ice Core data show abrupt climate change happens in few years. *Science* 321: 680–684.
- Wang YJ, Cheng H, Edwards RL et al. (2005) The Holocene Asian monsoon: Links to solar changes and North Atlantic climate. *Science* 308: 854–857.
- Wu WX and Liu TS (2004) Possible role of the “Holocene Event 3” on the collapse of neolithic cultures around the Central Plain of China. *Quaternary International* 117: 153–166.
- Yang B, Qin C, Braeuning A et al. (2021) Long-term decrease in Asian monsoon rainfall and abrupt climate change events over the past 6,700 years. *Proceedings of the National Academy of Sciences of the United States of America* 118(30): e2102007118.
- Yang X, Liu R, Zhang R et al. (2020) A stalagmite $\delta^{18}\text{O}$ record from Jinfo Cave, southern China reveals early-mid-holocene variations in the East Asian summer monsoon. *Quaternary International* 537: 61–68.
- Yang X, Yang H, Wang B et al. (2019) Early-Holocene monsoon instability and climatic optimum recorded by Chinese stalagmites. *Holocene* 29: 1059–1067.
- Zhang H, Brahim YA, Li H et al. (2019) The Asian summer monsoon: Teleconnections and forcing mechanisms—A review from Chinese speleothem $\delta^{18}\text{O}$ records. *Quaternary* 2(3): 26.
- Zhang H, Yin J, Cheng H et al. (2016) Discussion about the mechanism of the weak summer monsoon events during the early Holocene: A case study of precisely dated stalagmite record from Lianhua Cave, Hunan province, China. *Acta Sedimentologica Sinica* 34(2): 281–291 (in Chinese, with English abstract).
- Zhang R and Delworth TL (2005) Simulated tropical response to a substantial weakening of the Atlantic thermohaline circulation. *Journal of Climate* 18: 1853–1860.
- Zhang R, Yang X, Zhang H et al. (2021) Centennial- to millennial-scale Asian summer monsoon changes during the MIS 5/4 transition revealed by high-resolution stalagmite records from southwestern China. *Palaeogeography, Palaeoclimatology, Palaeoecology* 571: 110390.
- Zhang T, Li T-Y, Cheng H et al. (2017) Stalagmite-inferred centennial variability of the Asian summer monsoon in southwest China between 58 and 79 ka BP. *Quaternary Science Reviews* 160: 1–12.
- Zhang W, Yan H, Dodson J et al. (2018) The 9.2 ka event in Asian summer monsoon area: The strongest millennial scale collapse of the monsoon during the Holocene. *Climate Dynamics* 50: 2767–2782.
- Zhao J, Tan L, Yang Y et al. (2021) New insights towards an integrated understanding of NE Asian monsoon during mid to late-Holocene. *Quaternary Science Reviews* 254: 106793.
- Zhao Y, Liu Y, Guo Z et al. (2017) Abrupt vegetation shifts caused by gradual climate changes in central Asia during the Holocene. *Science China-Earth Sciences* 60: 1317–1327.
- Zickfeld K, Knopf B, Petoukhov V et al. (2005) Is the Indian summer monsoon stable against global change? *Geophysical Research Letters* 32: L15707.